POLITECNICO DI TORINO
Repository ISTITUZIONALE

A method to assess robustness of GPS C/A code in presence of CW interferences

(Article begins on next page)

05 May 2024

Research Article

A Method to Assess Robustness of GPS C/A Code in Presence of CW Interferences

Beatrice Motella,[1] Simone Savasta,[2] Davide Margaria,[2] and Fabio Dovis[2]

[1] *Navigation Lab, Istituto Superiore Mario Boella, via P.C. Boggio 61, 10138 Torino, Italy*
[2] *Dipartimento di Elettronica, Politecnico di Torino, C.so Duca degli Abruzzi 24, 10129 Torino, Italy*

Correspondence should be addressed to Davide Margaria, davide.margaria@polito.it

Navigation/positioning platforms integrated with wireless communication systems are being used in a rapidly growing number of new applications. The mutual benefits they can obtain from each other are intrinsically related to the interoperability level and to a properly designed coexistence. In this paper a new family of curves, called Interference Error Envelope (IEE), is used to assess the impact of possible interference due to other systems (e.g., communications) transmitting in close bandwidths to Global Navigation Satellite System (GNSS) signals. The focus is on the analysis of the GPS C/A code robustness against Continuous Wave (CW) interference.

1. Introduction

In the last years navigation technology is becoming essential for several civil applications, some of them even unthinkable at the time of the satellite navigation starting. Alongside the wide use in the transports fields (e.g., aviation, maritime, rail, and road), the range of civil uses is constantly increasing. Surveying, precision agriculture, environmental protection, scientific research (e.g., monitoring geological change, wildlife behaviour, atmospheric modelling, oceanic studies, space exploration), time-based applications (e.g., line power or telecommunications network synchronization and management) are examples of the most various applications based on the estimation of the user Position, Velocity, and Time (PVT).

This kind of applications, especially those devoted to safety, requires the coexistence of different communication systems and GNSS. The use of receivers able to provide multiple services, such as user position estimation and data transmission, embeds the problem of managing different systems with different specifications.

Despite Wireless Communication Systems (WCSs) use of different carrier frequencies with respect to GNSS bands, they could likewise represent potential threats for GNSS modules integrated in personal devices and communication units. This is due to the low-received GNSS signal power [1, 2], which makes the systems vulnerable to potential dangerous effects caused by undesired and unintentional interfering signals that might appear in the GNSS bandwidths. These interferences could compromise the correct functioning of the main blocks of the GNSS receiver chain, such as acquisition and tracking stages.

This fact would affect also the service based on the integrated communication/positioning system and might result in dangerous failures for those applications oriented to safety of life or as the ones involving financial transactions. For this reason, the development of strategies devoted to analyze and mitigate the impact of undesired signals that could compromise the correct integration of WCSs and GNSS receivers becomes crucial.

In this paper a tool for the evaluation of the potential receiver performance in presence of interfering signals is proposed. The strategy is based on a class of curves named Interference Error Envelope (IEE) and the derived Interference Running Average (IRA), able to assess the error made in the user position estimation due to the presence of an interference signal generated by some WCSs.

The paper is structured as follows. Section 2 gives an overview of real cases of GNSS malfunctioning due to presence of WCSs interference in GNSS bands. Sections 3 and 4 are dedicated to present the concepts of Interference Error Envelope and Interference Running Average and to explore the use of the IEE for assessing the GPS C/A code robustness. At the end some conclusions on the use of the proposed tools will be drawn.

2. Interference Impact on GNSS

It is well known that a GNSS receiver can be vulnerable to many classes of undesired signals. These disturbances can lead to a complete misbehaviour of the operational blocks in the receiver chain with consequences such as erroneous user position estimations or up to a full outage. This weakness is due to the low-power level of the Signal in Space (SIS) from which the pseudorange information is extracted (e.g., -158.5 dBW for GPS L1 C/A civil code [1] and -157 dBW expected for Galileo E1 [2]).

As a demonstration of interference vulnerability and jamming impact on GPS equipments, some trials have been recently conducted by the General Lighthouse Authorities of the United Kingdom and Ireland (GLA), in collaboration with the UK Ministry of Defence (MOD), Defence Science and Technology Laboratory (DSTL), aiming at assessing the effects of GPS jamming on safe navigation [3]. These trials demonstrated that when a GPS-equipped vessel enters in a jamming zone (area covered by an intentional jamming unit), numerous failures occur to systems based on GPS signals.

Every kind of communication system operating by frequencies near to the GNSS bands or with a high-power level with respect to GNSS, due to implementation imperfections, or to an inaccurate matching of the specifications, can affect the correct receiver functionalities. The presence of growing wireless communication infrastructures significantly increases the probability of spurious emissions in GNSS bands in some geographical area. An example of unintentional interference signal emissions is the malfunctioning of electronic devices (e.g.,: nonlinear amplifiers in TV transmitters) that might generate harmonics or intermodulation products.

In [4], the Digital Video Broadcasting—Terrestrial (DVB-T) system is analyzed as potential interference signal for both Galileo and GPS signals. Due to the high power transmitted, the harmonics of Orthogonal Frequency Division Multiplexing (OFDM) signal used in the DVB-T transmission have been analyzed, showing a degradation of the Carrier to density Noise ratio (C/N_0) up to 90 Km from the emitting sources.

In [5], an analysis of real interference sources in VHF and UHF bands is reported, highlighting how such kind of signals can partially or completely corrupt the GPS signal. Systems working at frequencies relatively far away from L1 band are explored as potential emitters in band by secondary harmonics.

Even if nonintentional Radio Frequency Interference (RFI) is not a priori predictable, several cases have been experienced in the past and reported in literature [6].

  (i) In 1994, in Germany, Digital Repeater transmissions at 1200 MHz degraded the C/N_0 in L2 band denying a correct acquisition of GPS signal [7].

 (ii) In 1995, both in Nice (France) and Vicenza (Italy), interferences related to secondary harmonics emitted by TV transmissions and microwave interference have been detected in GPS bands [7].

(iii) In 1995 at the Edinburg Airport (Germany), an interference due to a Distance Measuring Equipment (DME) transmitter caused a C/N_0 degradation [7].

(iv) In 1993, in the metropolitan Boston area (USA) an interference generated by TV emitters (Channel 10 and Channel 66) affected the quality of GPS signal forcing low C/N_0 with consequent tracking loss [7].

 (v) In April 2006, DVB spurious emission of TV transmitters located in Torino (Italy) degraded the performance in the acquisition stage of a GPS receiver operating in the area, with consequently loss of the GPS signal tracking [8]. The interference was the same that ESA researchers detected using the Galileo Experimental Tracking Receiver (GETR) with the GIOVE-A E1 signals at INRIM (Torino) [9].

(vi) In July 2006, UHF harmonics have been detected in Sidney around TV antennas. The undesired signal in the L1 band corrupted the correct performance of the receiver chain observing significant variations in the AGC/ADC block and in the final user positioning [10].

In several cases, due to the nature of emitted signals with respect to the GNSS bands, the interference can be modelled as pure Continuous Wave (CW), i.e. sinusoidal signals. This kind of RFI might saturate the first stage of receiver chain, such as the Low Noise Amplifier (LNA) or the Automatic Gain Control (AGC) for the Analog to Digital Conversion (ADC), or might lead to erroneous position estimations. Due to its spectral characteristics, as it will be shown in Section 4, this kind of interference is considered one of the most critical for the GPS C/A code [11].

It must be noticed that the choice of using the CW interference as a model for WCSs do not prevent from drawing general conclusions on the interference vulnerability due to other interference sources. In fact, as already noticed by the authors in [12] and [13], IEE curves obtained with a CW interference can be easily used to predict the behaviour of the receiver in presence of different interfering sources (e.g., wideband interferences, applying a moving average on the CW IEE).

Next Section is then devoted to the introduction of the concepts of IEE and IRA curves.

3. Interference Impact Assessment Tools

Although the impact of CW interferences on GNSS receivers is a topic already approached in different publications, only in some cases theoretical and/or simulative models for the interference impact have been derived. In [14], a theoretical formula for the code tracking bias due to Continuous Wave interference has been introduced. In order to take into account also the receiver front-end filtering effect, in assessing the interference impact on receiver performance, a novel method (intended as both an analytical and simulative framework) has been recently defined by the authors in [12, 13].

A new family of curves, named Interference Error Envelope (IEE), is introduced as a reliable tool for evaluating the potential GNSS receiver performance in terms of potential positioning error due to the presence of interfering signals, varying one or more parameters of the interference (e.g., the carrier frequency for a CW signal) and/or the receiver setup (e.g., integration time, bandwidth, discriminator type, correlator spacing).

The IEE curves are based on a concept similar to that used for the well-known Multipath Error Envelopes (MEE, see [15]): the idea is to measure the worst-case distortion of the discrimination function when the useful SIS is affected by a specific type of interference.

Figure 1 shows a qualitative example of how the presence of an interference might distort a coherent discrimination function obtained with a GPS L1 (Binary Phase Shift Keying—BPSK modulation) signal. In this case the interferer is modelled as a CW signal, with the carrier frequency centred at 0.5 MHz from the GPS L1 carrier. Due to the CW, the code discrimination function in Figure 1 is distorted and a bias can be noticed in the zero-crossing (Delay Look Loop tracking point), leading to a ranging error.

A detailed theoretical analysis of the interference impact on GNSS receivers can be found in [13]. In general, assuming a received signal affected by a generic interference signal $i(t)$ at a frequency shift f_i with respect to signal carrier frequency, the maximum bias (b_{max}) on the zero-crossing point of the discrimination function can be computed as

$$b_{max}(f_i)$$
$$= \alpha \cdot \frac{2}{ML} \int_{-\infty}^{\infty} |I(f)| \, |W(f)| \, |C(f)| \sin(\pi f \Delta) df, \tag{1}$$

where

- (i) $\alpha = -(c \cdot T_C \cdot \Delta)/2$, being c is the speed of light, T_C the code chip duration, and Δ the Early-Late spacing;
- (ii) L is the length of a code period in samples and M is the number of integration periods in the coherent integration time for computing the correlation values;
- (iii) $I(f)$ is the Discrete Time Fourier Transform (DTFT) of the interference signal $i(t)$: $I(f) = \text{DTFT}\{i(nT_s)\}$;
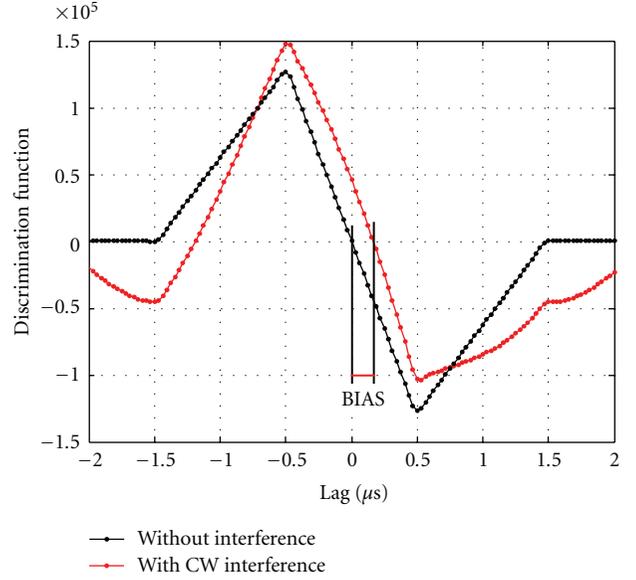

FIGURE 1: GPS L1 signal (BPSK) discrimination function distortion due to the presence of a CW interference (coherent Early-Late discriminator with 1 chip spacing, integration time equal to 4 ms).

- (iv) $W(f) = \text{DTFT}\{w(nT_s)\}$, being $w(nT_s)$ the discrete time impulse response modeling the receiver front end;
- (v) $C(f) = \text{DTFT}\{c(nT_s)\}$, being $c(t)$ the code chip sequence, including also the SIS modulation.

In case of a CW interference at a frequency shift f_i, $|I(f)|$ can be modeled as

$$|I(f)| = A \cdot \delta(f - f_i) \tag{2}$$

where A is the amplitude of the CW interference.

Substituting (2) in (1), the maximum bias b_{max}^{CW} in presence of a CW interference can then be expressed as

$$b_{max}^{CW}(f_i) = \alpha \cdot \frac{2A}{ML} |W(f_i)| \, |C(f_i)| \sin(\pi f_i \Delta). \tag{3}$$

It is important to remark that in (1) and (3) the maximum distortion of the discrimination function depends not only on the features of the interference and the received signals, but also on the receiver setup (integration time, front-end filter, correlator spacing). For the complete derivation and validation of previous equations please refer to [13], where the generalization in case of wideband interferences is also presented.

The IEE is then defined as a measure of the maximum distortion of the discriminator function with respect to one (or more) parameter of the interfering signal: the worst cases corresponding to the maximum and minimum ranging error values (expressed in meters) are plotted versus one of the variable interference characteristics being considered (e.g., the carrier frequency for a continuous wave interferer) [12, 13].

The main innovation of the IEE and IRA curves with respect to other interference assessment methods is that they
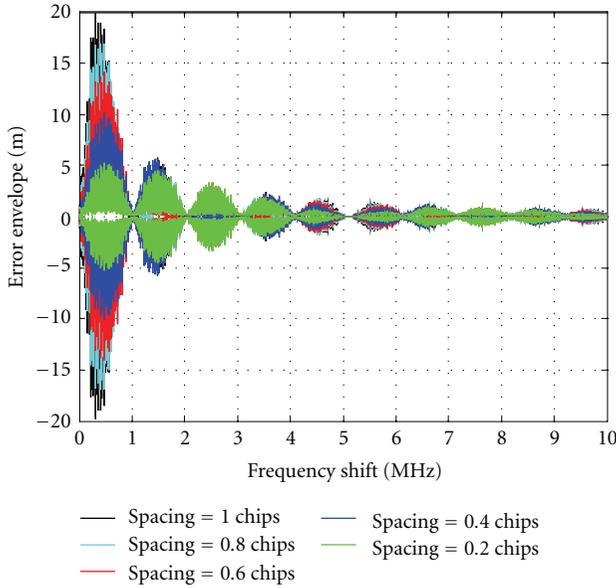
FIGURE 2: Interference Error Envelope comparison in presence of a CW interference obtained for a coherent Early-Late discriminator with different correlator spacings (from 0.2 to 1 chip) with a BPSK (GPS L1) signal.


FIGURE 3: Interference Error Envelope in presence of a CW interference obtained for a coherent Early-Late discriminator with a correlator spacing of 0.4 chip with a BPSK signal.

are not limited to the analysis of the received signal features, allowing detailed analysis on specific interference parameters also taking into account the receiver setup.

As an example, in order to better understand the idea the method is based on, some IEE curves are depicted in Figure 2. In this case the effect of a CW interference on the GPS L1 signal (Binary Phase Shift Keying—BPSK modulation) is assessed, considering a coherent Early-Late discriminator with different correlator spacings (from 1 to 0.2 chips).

This plot has been obtained simulating a carrier to interference power ratio equal to 0 dB (same power for the useful SIS and the CW interference). The carrier frequency of the CW sweeps from 0 to 10 MHz with respect to the GPS L1 carrier frequency and its phase has been varied from 0 to 2π.

The IEE curves in Figure 2 have then been obtained considering the maximum and the minimum values (over all the possible phases) of the ranging errors versus the CW carrier frequency (the x axis represents the offset between the CW and the GPS carrier frequency). In this way a useful tool for assessing the worst-case errors (maximum and minimum) for each CW carrier frequency is provided.

From this kind of analysis and plots the ranging errors due to a specific interference can be easily evaluated. Observing Figure 2, the error envelopes present symmetry between positive and negative values with a shape similar to the BPSK spectrum. It is possible to notice that for large values of the correlator spacing the IEE curves present high-ranging errors while they decrease with the reduced Early-Late distance. But in all the cases the CW interference is more harmful if its carrier frequency is around 0.5 MHz
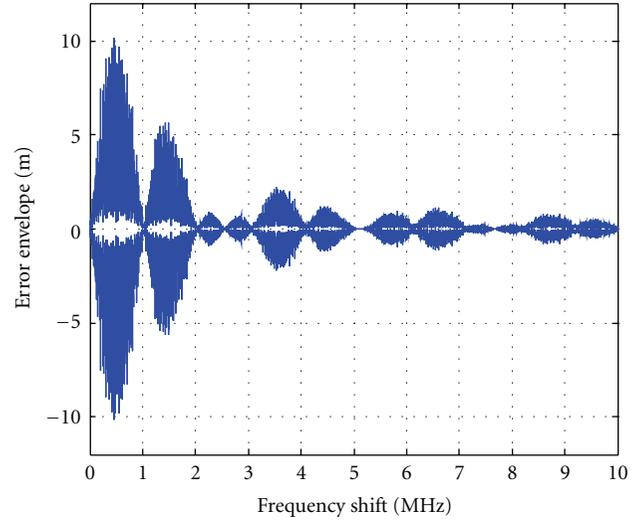
(corresponding to the half of the main lobe of the spectrum) and then its impact decreases moving away from the central frequency.

The shape of the IEE and the resulting performance also depend on the characteristics of the specific PRN code being considered, as it will be discussed in Section 4. The zeros of Figure 2 depend on the modulation of two different contributes of (3) the following:

(i) The code elementary function, contained in the DTFT $C(f)$. In case of a BPSK signal the contribute is a sinc function with zeros defined by the inverse of the chip period T_c. Notice that in case of a BOC(1,1) modulation, the zeros position is different from the BPSK case since the chip shaping is defined by the combination of a sinc and a sine profile with period $1/T_c$ [13].

(ii) The sine function (dependent on the spacing Δ). It introduces zeros accordingly to its period.

To show the modulation effect on the zeros placement due to the two contributes, the IEE of a CW in case of spacing $\Delta = 0.4$ is reported in Figure 3. In this case two zeros at 2.5 MHz and 7.5 MHz are added to the zeros observed at entire multiple of 1.023 MHz.

An alternative way to show the described results is the Interference Running Average (IRA) curves, obtained averaging the IEE and representing the potential average impact of an interference whose carrier frequency is uniformly distributed in a chosen frequency range [13]. The IRA curves do not add information to the analysis performed using the IEE, but provide a simplified representation of the receiver performance, allowing an easy comparison of interference vulnerability for different receiver configurations.

The IEE curves, together with the corresponding IRA curves, are a reliable quantitative method that can be used in order to assess and compare the interference robustness

level of different GNSS signals. Some examples of analysis already performed by means of IEE are provided in [12, 13], where the impacts of both continuous wave and wide band interference are assessed, performing a full comparison between different GNSS modulations (BPSK, BOC, CBOC, and TMBOC) and considering different receiver configurations. Referring to the concepts introduced in this Section, the paper focuses the attention on the GPS C/A code.

While in [12, 13] the IEE is used to compare the interference robustness among different modulation types and vary the receiver configuration, here the performed analysis is focused on comparing the robustness among the GPS C/A PRN codes by varying the CW carrier frequency.

The final goal is to identify the worst case (i.e., the most dangerous CW carrier frequency) for each specific GPS satellite signal.

4. Impact on IEE of the GPS C/A Code Lines

The GPS C/A code signal is based on the Gold code characteristics [1]. Such signal has a line spectrum (neglecting the navigation data) with lines at 1 kHz from each other. Moreover, depending on the code, there are some lines that are stronger [11]. This means that a CW jammer might mix with a strong C/A code line and leak through the correlator, affecting the receiver performance or even preventing the correct functioning of the receiver. Three facts must be pointed out:

  (i) Because of the C/A code signal structure, CWs might be very harmful sources of interference [11];

  (ii) Such a harmfulness is strictly related with the relative position between the CW carrier frequency and the code strongest line [16];

  (iii) Also the relative carrier phase can have an impact.

From [17], the Power Spectral Density (PSD) of the C/A code signal spectrum can be expressed as

$$S_{\text{C/A}} = \frac{T_b}{(NT_C)^2} |C(f)|^2 \sum_{l=-\infty}^{\infty} \text{sinc}^2\left[T_b\left(f - \frac{l}{NT_C}\right)\right],$$

(4)

where

  (i) $|C(f)|^2 = T_C^2 N \cdot \text{sinc}^2(fT_C) \cdot |X_{\text{code}}(f)|^2$;

  (ii) $X_{\text{code}}(f)$ is the Discrete Time Fourier Transform of x_n: $X_{\text{code}}(f) = \sum_{n=0}^{N-1} x_n e^{j2\pi fnT_C}$;

  (iii) $\{x_n\}_{n=0}^{N-1}$ is the binary Gold code sequence;

  (iv) $T_C = 0.976\,\mu s$ is the code chip duration;

  (v) $N = 1023$ is the number of chips in 1 code period;

  (vi) $T_b = 20 \cdot N \cdot T_C = 20$ ms is the data bit duration.

It must be remarked that $S_{\text{C/A}}$ in (4) is composed by three functions in the frequency domain:

  (i) $\text{sinc}^2(fT_C)$, due to the rectangular code chip;
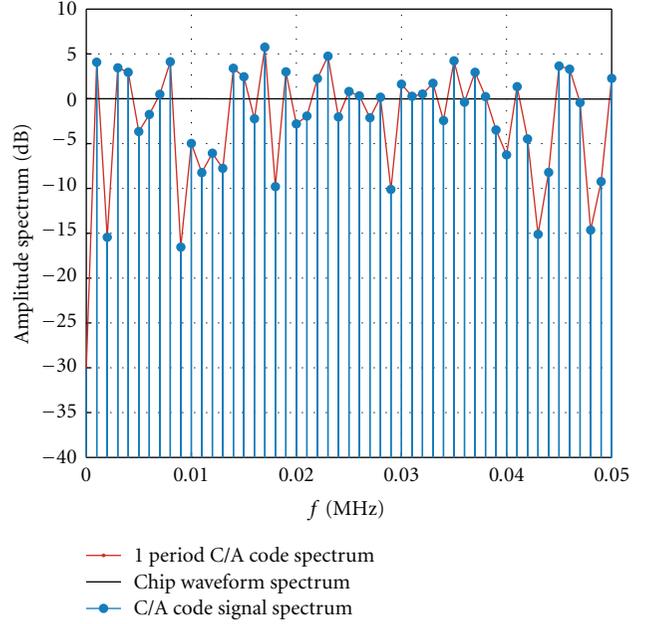
FIGURE 4: Spectrum of 1 period of the PRN 23 C/A code (orange line), chip waveform spectrum (solid black line), and PRN 23 C/A code signal spectrum (solid cyan line).

  (ii) $X_{\text{code}}(f)$ which is the DTFT of the Gold code;

  (iii) The third term is due to the code repetition and consists of a comb of sinc functions, at 1 kHz from each other.

All these three components are clearly depicted in Figure 4.

It is also possible to appreciate the three frequency functions by changing the resolution bandwidth to a spectrum analyzer linked with a RF GPS signal generator. The effect is shown in Figure 5, where the GPS C/A code spectrum is depicted tuning the resolution bandwidth at 100 kHz, 1 kHz, and 100 Hz, respectively.

The difference in terms of energy carried by each line can be noticed in Figure 6, where the spectrum of the C/A code signal is depicted for two different codes (PRN 7 and 23).

In terms of interference robustness, the strongest line for each C/A code can be called *worst line*, since it is more susceptible to interference. Table 1 lists all the PRN codes worst lines [11].

One of the tests that has been performed using the IEE tool (see Section 3) verifies that, after fixing the CW frequency shift and evaluating the IEE for each PRN code, the maximum IEE is obtained for the PRN having the strongest line coincident with the CW shift, as reported in Table 2.

The double check between Table 1 and Table 2 confirm the test. All the PRN worst line combinations correspond. Only two facts have to be remarked:

  (i) For CW at 151 kHz, the maximum IEE corresponds to PRN 9, instead of PRN 25. This is because the strongest line of PRN 25 and the sixth strongest line of PRN 9 have practically the same amplitude (−23.78 and −23.81 dB);
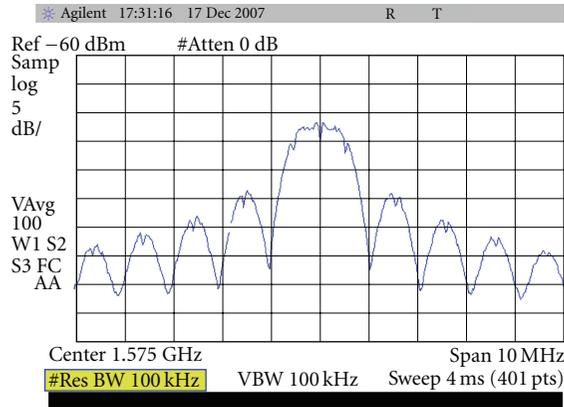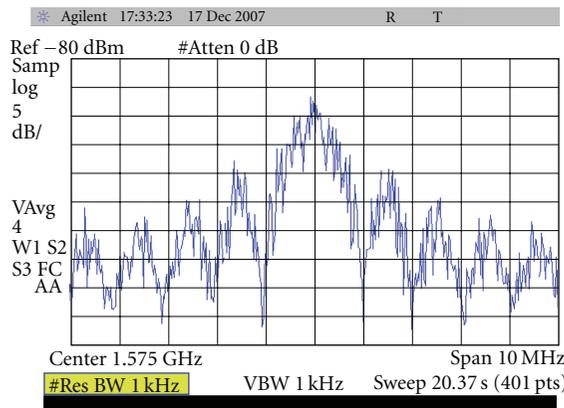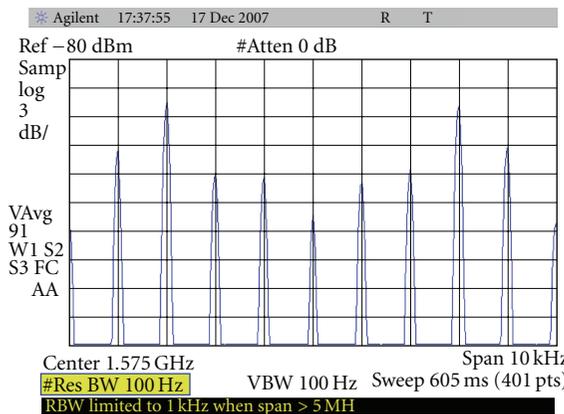
Figure 5: PSD evaluated by the ESA-E series Agilent 4402B spectrum analyzer, with a resolution bandwidth of 100 kHz, 1 kHz and 100 Hz, respectively.

(ii) Both the PRN 4 and PRN 11 have the strongest line at 122 kHz. The maximum IEE at this frequency corresponds to PRN 11. This fact is confirmed by the two line amplitudes: -22.98 dB for the PRN 4 and -22.64 dB for PRN 11.

Using the IEE curves, it is possible to define *new worst lines* for the specific receiver configuration (taking into

Table 1: GPS C/A Code Worst Lines for Prn 1 to 32.

C/A code PRN #	Worst Line Frequency [kHz]	C/A code PRN #	Worst Line Frequency [kHz]
1	42	17	138
2	263	18	183
3	108	19	211
4	122	20	30
5	23	21	55
6	227	22	12
7	78	23	127
8	66	24	123
9	173	25	151
10	16	26	102
11	122	27	132
12	199	28	203
13	214	29	176
14	120	30	63
15	69	31	72
16	154	32	74

Table 2: Analysis of Code Lines from IEE Maximum.

CW frequency shift [kHz]	PRN (IEE max)	CW frequency shift [kHz]	PRN (IEE max)
12	22	122	11
16	10	123	24
23	5	127	23
30	20	132	27
42	1	138	17
55	21	151	9
63	30	154	16
66	8	173	9
69	15	176	29
72	31	183	18
74	32	199	12
78	7	203	28
102	26	214	13
108	3	221	19
120	14	227	6
		263	2

account the discriminator setting, the front end filter type and bandwidth).

The new worst-case frequencies lines are listed in Table 3. They have been obtained simulating an infinite bandwidth signal with a coherent discriminator (Early-Late with spacing 1 chip).

Referring to first line in Table 3, Figure 7 provides an example of the procedure followed for the definition of the new worst line on the IEE obtained simulating the PRN 1.

It is important to point out that the definition of *"new" worst lines* changes the point of view in assessing the interference impact. This definition points out that the strongest code line can also not be the worst one.

In fact the new definition is receiver dependent, since the impact of a CW interferer is related to several factors:

(i) CW characteristics, that is, power, carrier frequency, phase;
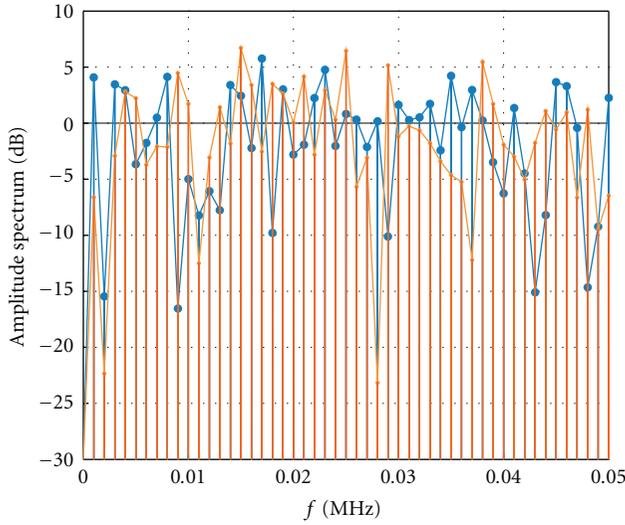
FIGURE 6: PRN 7 (orange) and PRN 23 (cyan) C/A code signal spectra.
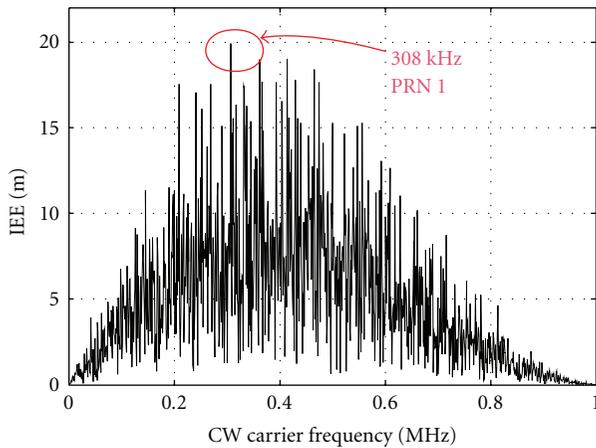
FIGURE 7: Definition of the new GPS C/A code worst line on the IEE for the PRN 1.

(ii) Specific code features (PRN number);

(iii) Receiver characteristics, that is, discriminator spacing, and front end parameters (filter, ADC, AGC, etc.).

As an example of the dependence of the IEE on the receiver setup, an additional analysis has been carried out in order to assess the impact of the discriminator spacing on the new worst lines. In detail the GPS C/A PRN 1 signal has been simulated with infinite bandwidth and processed by using a coherent Early-Late discriminator with different correlator spacings (from 0.2 to 1 chip). Figure 8 shows a zoom on Figure 2, aiming at investigating the impact of the spacing on the worst case error in presence of CW interference. The obtained results in terms of worst lines are summarized in Table 4. As already remarked in Section 3, these results confirm that a reduction of the spacing decreases the magnitude of the envelope errors.

TABLE 3: "New" GPS C/A Code Worst Lines.

C/A code PRN #	Worst Line Frequency (kHz)	C/A code PRN #	Worst Line Frequency (kHz)
1	308	17	434
2	402	18	456
3	447	19	394
4	456	20	461
5	381	21	453
6	347	22	364
7	376	23	438
8	435	24	384
9	354	25	257
10	443	26	417
11	397	27	441
12	410	28	355
13	412	29	433
14	369	30	426
15	338	31	423
16	423	32	376

TABLE 4: Worst Lines for GPS C/A PRN no. 1 varying the Discriminator Spacing.

Coherent Early-Late Discriminator Spacing (chips)	Worst Line Frequency (kHz)	IEE max (m)
1	308	19.91
0.8	466	16.94
0.6	466	14.13
0.4	466	10.16
0.2	466	5.30

In addition, it is possible to notice that, by varying the spacing, the worst lines can match different frequencies. In detail, the worst line is at 308 kHz only for a spacing of 1 chip, whereas other spacings lead to a different interference vulnerability, showing a worst line at 466 kHz. It must be remarked that these results have been obtained simulating a BPSK modulated signal (GPS C/A code). Obviously different results are expected considering other signals (e.g., BOC modulated), featuring a larger spectral occupation, or different PRN codes, leading to different worst lines.

Finally, it must be remarked that, as noted in [12, 13], CW analysis is the base for predicting results also in presence of larger bandwidth interference (wideband signals), that might affect more than one line at the time.

5. Conclusions

The increasing number of application based on the integration of wireless communications and navigation/localization techniques leads to the need to verify their interoperability. Within this scenario, the assessment of the GNSS interference robustness is one of the most sensitive issues.

An innovative quantitative method to measure the interference impact for GNSS signals has been described in the paper. It consists in evaluating the distortion of the discrimination function produced by the presence of
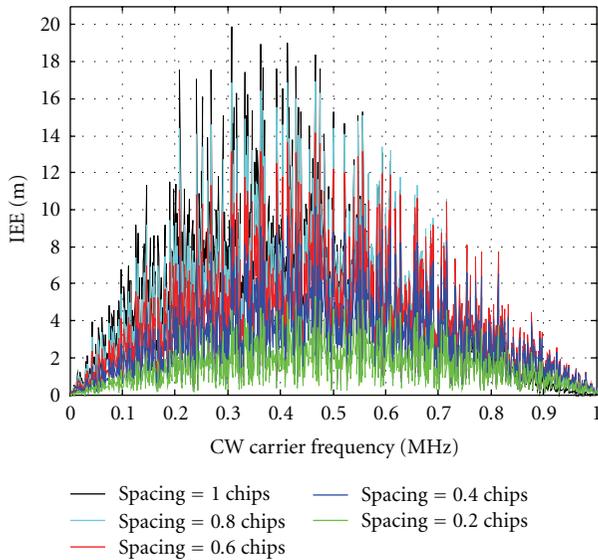
FIGURE 8: Comparison of IEE curves obtained varying the coherent Early-Late discriminator spacing (zoom on Figure 2).

the interference and can be customized for each type of disturbance. A new family of curves, the *Interference Error Envelope*, has been introduced. Each IEE measures the maximum correlation distortion versus the specific interferer characteristic being considered (e.g., the carrier frequency for a continuous wave interferer), for a specific receiver setting.

Moreover the paper presented a detailed analysis on the effect of CW interference on the different GPS C/A codes. Starting from the concept of worst line (the strongest line for each code), and exploiting the IEE tool, *new worst lines*, that also take into account the receiver architecture, have been found.

References

[1] Interface Specification, IS-GPS-200 Rev.D, IRN-200D-001, 7 March 2006.

[2] Galileo Signal In Space Interface Control Document (OS SIS ICD), Draft 1, February 2008, http://www.gsa.europa.eu.

[3] A. Grant, P. Williams, N. Ward, and S. Basker, "GPS jamming and the impact on maritime navigation," *Journal of Navigation*, vol. 62, no. 2, pp. 173–187, 2009.

[4] D. Borio, S. Savasta, and L. L. Presti, "On the DVB-T coexistence with Galileo and GPS systems," in *Proceedings of the 3rd ESA Workshop on Satellite Navigation User Equipment Technologies (NAVITEC '06)*, ESA/ESTEC, Noordwijk, The Netherlands, December 2006.

[5] R. J. Landry and A. Renard, "Analysis of potential interference sources and assessment of present solutions for GPS/GNSS receivers," in *Proceedings of the 4th International Conference on Integrated Navigation Systems*, pp. 1–13, 1997.

[6] John A. Volpe National Transportation Systems Centre, "Vulnerability assessment of the transportation infrastructure relying on the global positioning system," Final Report, US Department of Transportation, Washington, DC, USA, August 2001.

[7] E. Backer, D. Van Willigen, and R. Rawlings, "Technical and operational assessment of the suitability of GPS to meet the BRNAV requirements," Tech. Rep., Delft University of Technology Telecommunications and Traffic Control Systems Group, Delft, The Netherlands, August 1997.

[8] B. Motella, M. Pini, and F. Dovis, "Investigation on the effect of strong out-of-band signals on global navigation satellite systems receivers," *GPS Solutions*, vol. 12, no. 2, pp. 77–86, 2008.

[9] P. F. De Bakker, J. Samson, P. Joosten, M. Spelat, M. Hollreiser, and B. Ambrosius, "Effect of radio frequency interference on GNSS receiver output," in *Proceedings of the 3rd ESA Workshop on Satellite Navigation User Equipment Technologies (NAVITEC '06)*, Noordwijk, The Netherlands, December 2006.

[10] A. T. Balaei, B. Motella, and A. G. Dempster, "GPS interference detected in Sydney-Australia," in *Proceedings of the International Global Navigation Satellite Systems Society conference (IGNSS '07)*, Sydney, Australia, December 2007.

[11] E. D. Kaplan and C. J. Hegarty, *Understanding GPS: Principles and Applications*, Artech House, Norwood, Mass, USA, 2nd edition, 2006.

[12] B. Motella, S. Savasta, D. Margaria, and F. Dovis, "An interference impact assessment model for GNSS signals," in *Proceedings of the 21st International Technical Meeting of the Satellite Division of the Institute of Navigation (ION GNSS '08)*, vol. 4, pp. 900–908, Savannah, Ga, USA, September 2008.

[13] B. Motella, S. Savasta, D. Margaria, and F. Dovis, "A method for assessing the interference impact on GNSS receivers," *IEEE Transactions on Aerospace and Electronic Systems*. In press.

[14] A. Martineau, *Performance of receiver autonomous integrity monitoring (RAIM) for vertically guided approaches*, Ph.D. thesis, 2008.

[15] M. Irsigler, J. A. Avila-Rodriguez, and G. W. Hein, "Criteria for GNSS multipath performance assessment," in *Proceedings of the 18th International Technical Meeting of the Satellite Division of The Institute of Navigation (ION GNSS '05)*, Long Beach, Calif, USA, September 2005.

[16] A. T. Balaei, B. Motella, and A. Dempster, "A preventative approach to mitigating CW interference in GPS receivers," *GPS Solutions*, vol. 12, no. 3, pp. 199–209, 2008.

[17] P. Misra and P. Enge, *Global Positioning System. Signal Measurements and Performance*, Ganga-Jamuna Press, Lincoln, Mass, USA, 2nd edition, 2006.